Improving effect of metal and oxide nanoparticles encapsulated in porous silica on fermentative biohydrogen production by *Clostridium butyricum*

Laurent Beckers *[, a], Serge Hiligsmann [a], Stéphanie D. Lambert [b], Benoît Heinrichs [b], Philippe Thonart [a]

* Corresponding author:

Email address: beckers.laurent@gmail.com

Tel.: +32 (0) 4 366 28 61

Fax: +32 (0) 4 366 28 62

[a] Centre Wallon de Biologie Industrielle (CWBI), Département des Sciences de la Vie, B40, Université de Liège, B-4000 Liège, Belgium.

[b] Laboratoire de Génie Chimique, B6a, Université de Liège, B-4000 Liège, Belgium.

Abstract

This paper investigated the enhancement effect of nanometre-sized metallic (Pd, Ag and Cu) or metallic oxide (Fe_xO_y) nanoparticles on fermentative hydrogen production from glucose by a *Clostridium butyricum* strain. These nanoparticles (NP) of about 2-3 nm were encapsulated in porous silica (SiO_2) and were added at very low concentration (10^{-6} mol·L^{-1}) in batch hydrogen production test. The cultures containing iron oxide NP produced 38% more hydrogen with a higher maximum H_2 production rate (HPR) of 58% than those without NP or with silica particles only. The iron oxide NP were used in a 2.5 L sequencing-batch reactor and showed no significant effect on the yields (established at 2.2 $mol_{hydrogen}\cdot mol_{glucose}^{-1}$) but an improvement of the HPR (+ 113%, reaching a maximum HPR of 86 $mL_{hydrogen}\cdot L^{-1}\cdot h^{-1}$). These results suggest an improvement of the electron transfers trough some combinations between enzymatic activity and inorganic materials.

Keywords: biohydrogen; dark fermentation; Clostridium butyricum; encapsulated nanoparticles; sol-gel process.

1. Introduction

In the upcoming years, the population living on our planet will increase and they will have to be provided with enough energy, materials and food. Currently, our society is based on the utilization of fossil fuels as a primary energetic source leading the world to environmental, human health and macro-economic issues (Zidansek *et al.*, 2009). The development of alternative and green energy sources is therefore regarded as a major answer aiming to lower the impact of the human industrial activity on the earth. In this context, it is believed that hydrogen will be used extensively in the future as an energetic vector to achieve a less polluting and economically more advantageous society than the current fossil fuel-based economy (Marban & Vales-Solis, 2007). Indeed, its reaction with oxygen, which produces energy and only water as a side-product, can be performed in electrochemical or combustion processes without any generation of greenhouse gases. However, currently, hydrogen is almost exclusively produced from traditional non-renewable fossil fuels in intensive chemical processes, running at elevated pressures and temperatures and releasing CO_2 in the atmosphere (Holladay *et al.*, 2009).

The green hydrogen produced by microorganisms provides alternative routes for renewable energy production (Kothari *et al.*, 2012). Among the several microorganisms that can convert various carbohydrate sources in hydrogen and metabolites in solution, the anaerobic fermentative bacteria have been studied during the past few years (Davila-Vazquez *et al.*, 2008; Hallenbeck, 2009). In these microorganisms, the electrons resulting from the oxidation of the substrate are transferred to protons in order to form molecular hydrogen through the action of enzymes called hydrogenases. Among the anaerobic bacteria producing hydrogen,

Clostridium strains are frequently characterised in highly efficient sludge for hydrogen production in mesophilic range of temperatures (Sagnak et al., 2010; Wang & Wan, 2009a). To date, the anaerobic biohydrogen process is still experimented at laboratory or small pilot scale only (Das, 2009). To make the process viable, improvements of the bioactivity of hydrogen-producing microorganisms as well as high substrate conversion yields are needed to meet economic requirements. Key factors for optimal hydrogen production such as pH, temperature, strain selection, microorganisms cell density, concentration of substrate and metabolites have been well studied to improve the kinetics and the yields (Davila-Vazquez et al., 2008; Wang & Wan, 2009a). However, further efforts and new routes have to be found to use these microorganisms more efficiently in a stable process.

Recently, the nanoscience has been involved in number of usual products and processes since the nanomaterials bring new chemical and physical properties. Indeed, due to their size between 1 and 100 nm, the nanomaterials exhibit a very large specific surface area and quantum effects start to predominate (Dinesh *et al.*, 2012). The interest in the biological field is still increasing with practical application in many different domains since nanoparticles (NP) have recently showed interactions with microorganisms even at very low concentration. On the one hand, some NP exhibit antimicrobial activity by close contact with the microorganisms leading to membrane disruption, also raising environmental concerns about their dissemination in the nature (Neal, 2008). On the other hand, some microorganisms may take advantages of NP especially in anaerobic environment, by transferring more efficiently electrons to acceptors. Intra- or extra-cellular NP may be produced by the reduction of metal ions for the biosynthesis of nanomaterials with different chemical composition or morphologies (Korbekandi *et al.*, 2009). Electron transfer can also occur through membrane *c*-type cytochromes or nanowires to electron acceptors such as polluting chemical compounds (for soil remediation applications (Jagadevan *et al.*, 2012)), electrodes (for current generation

in microbial fuel cells (Lovley, 2008)) or through interspecies electron transfer (Kato *et al.*, 2012). In all these application fields, the NP have recently shown some advantages through their capacity to react rapidly with the electron donors leading therefore to kinetic improvement and, through their action as biocatalysts, to the enhancements of the microorganisms activity (Xu *et al.*, 2012).

In a previous work, only gold NP at very low concentration (10^{-8} mol·L^{-1}) were tested to observe effects on the biohydrogen production. An enhancement of the performances of about 56% was achieved (Zhang & Shen, 2007). The authors concluded that gold NP would operate as "electron sinks" due to their affinity for electrons, which allows to further reduce protons to hydrogen. They acted in parallel on hydrogenases that naturally achieve this reaction in the metabolism of the cell. Other metal are known to interact with microorganisms in environmental conditions. Ag and Cu are often cited as metal having interaction with the bacteria for their antimicrobial activity (Bagchi et al., 2012; Sotiriou & Pratsinis, 2010). Pd is a metal involved usually for its strong interactions with molecular hydrogen in chemical processes (Klavsyuk *et al.*, 2011). Finally, iron is known to be an important element as a cofactor for hydrogenases or for its role in environmental processes (Grieger *et al.*, 2010; Lee *et al.*, 2001; Xu *et al.*, 2012).

In this work, the effect of nanoparticles (NP) of about 2-3 nm of three metals (Pd, Ag, Cu) and one iron (Fe) oxide was investigated with pure *Clostridium butyricum* cultures. These NP were encapsulated in a porous silica (SiO_2) matrix. The SiO_2 matrix without NP was also tested in the same conditions. To synthesize the catalyst (NP + SiO_2 = catalyst), a one-step sol-gel process was applied to obtain NP finely dispersed in the porosity of a silica matrix (Heinrichs *et al.*, 2008; Lambert *et al.*, 2004). In such catalysts, in order to reach active sites, reactants must first diffuse through large pores located between aggregates of SiO_2 particles and then through smaller pores between those elementary particles inside the aggregates.

Finally, they diffuse through micropores inside the silica particles. It was shown that there are no limitations of mass transfer at each of the three levels (Heinrichs *et al.*, 2001).

These NP were experimented in Biochemical Hydrogen Potential (BHP) tests. The most efficient conditions were further investigated in a stirred 2.3 L Anaerobic Sequenced-Batch Reactor (AnSBR). The production of hydrogen and metabolites was monitored in the cultures and the Gompertz model was applied on the volumetric production curves.

2. Material and methods

2.1. Microorganism and culture medium

The strain used as hydrogen-producing microorganism was *Clostridium butyricum* CWBI1009 (denoted *C. butyricum*) and was previously isolated and identified by the authors (Masset *et al.*, 2010). It was conserved by sterile monthly transfer of 1 mL from previous pure culture in a hermetically sealed 25 mL tubes containing “MDT” medium and incubated at 30°C. The MDT culture medium contained, per litre of deionized water: glucose monohydrate (5 g), casein peptone (5 g), yeast extract (0.5 g), Na_2HPO_4 (5.1 g), KH_2PO_4 (1.2 g), $MgSO_4.7H_2O$ (0.5 g) and L-cysteine hydrochloride (0.5 g). The MDT culture medium was used in biochemical hydrogen potential (BHP) batch serum bottles test and in 2.5L stirred tank reactor driven in anaerobic sequenced-batch mode (AnSBR).

For the preparation of fresh inoculum, the transfer in new MDT tubes was repeated twice a week before being used in the culture vessel. Purity tests were performed by spreading 100 µL of culture on sterile PCA (Plate Count Agar) Petri dishes before incubation at 30°C for 24 to 48 hours. The PCA medium contained glucose monohydrate (1 g), casein peptone (5 g), yeast extract (2.5 g) and agar (15 g) per litre of deionized water. The absence of bacterial growth after incubation for 48 h incubation confirmed the absence of any facultative anaerobic contaminants.

2.2. Preparation and characterization of encapsulated nanoparticles

Four metallic salts (Pd, Ag, Cu and Fe) have been used for preparing the nanoparticles (NP). To encapsulate these NP inside a porous silica matrix, the cogelation method was used as described by Lambert *et al.* (Lambert *et al.*, 2004) and by Heinrichs *et al.* (Heinrichs, 2008). The samples are denoted Pd/SiO_2, Ag/SiO_2, Cu/SiO_2 and Fe/SiO_2 cogel (Table 1). The cogelation method allows doping an inorganic matrix with cations, in one step at the molecular scale. The process is based on the simultaneous hydrolysis and condensation of two alkoxysilanes: an SiO_2 network-forming reagent such as tetraethoxysilane (TEOS, $Si(OC_2H_5)_4$) and an alkoxysilane-functionalized ligand of the type $(RO)_3Si$-X-L, in which the ligand L, able to form a complex $-L_nM$ with a cation of a metal M (M = Pd, Ag, Cu, Fe etc.), is connected to the hydrolysable alkoxide group $(RO)_3Si$- via an inert and hydrolytically stable spacer X. The concomitant hydrolysis and condensation of such molecules, *i.e.* their cogelation, results in materials in which the catalytic metal cation is anchored to the silica matrix.

In Table 1, a second Fe/SiO_2 sample, called Fe/SiO_2 dissol, is presented. This sample was prepared by the dissolution method (Heinrichs, 2008), which consists of dissolving the iron salt in the initial homogenous solution of silica gel precursor. Moreover, the porous silica matrix without NP, denoted SiO_2 , was also synthesized by the sol-gel process (Lambert, 2004) to check if SiO2 plays a significant rule for the biohydrogen production.

All these samples were calcined under air (550°C for Fe/SiO_2 dissol and Fe/SiO_2 cogel, 400°C for the other samples) to remove organic moieties. After the calcination step, Pd/SiO_2, Ag/SiO_2 and Cu/SiO_2 were reduced under H_2 to obtain metallic NP (Lambert, 2004).

The samples were characterized (textural analysis, electron microscopy, X-ray diffraction) by using the methods described by (Lambert *et al.*, 2004) and (Heinrichs *et al.*, 2008). For the clarity of this work, NP is defined as metallic or metallic oxide nanoparticules highly

dispersed inside the silica matrix, whereas catalyst is used to define the combination between NP and silica.

Concentrated suspensions in water of these samples were prepared in 50 mL bottles by finely pounding (at micrometre-size) and weighting some catalysts. Based on the mass suspended in the bottles, the metallic mass loading in the catalyst and the metal atomic weight (Table 1), a defined volume of homogenized suspension was transferred in the culture medium prior to sterilization in order to reach a final concentration of 10^{-6} $mol_{metal} \cdot L^{-1}$. Therefore, all the tests had the same NP concentration, but the total mass of catalyst (*i.e.* NP + SiO_2) differed from one test to the others, because the metallic mass loading differs between the investigated catalysts. An equivalent mass of SiO_2 was added in the corresponding test without NP.

2.3. <u>Fermentation set-up</u>

The BHP tests were carried out in 270 mL bottles with 200 mL of MDT medium adjusted at pH 7.6 with NaOH 5N as formerly described by (Hamilton *et al.*, 2010). Suspended catalysts were added in the bottles to reach the wished metallic concentration prior to sterilization. The bottles were inoculated with 3 mL of inoculum before being capped tightly with a sterile rubber septum, flushed with sterile nitrogen and incubated at a temperature of 30 °C. The data for the BHP test are representative results of independent experiments run in triplicates.

The experiments in AnSBR were done in a 2.5 L laboratory-scale tank bioreactor (Biolafite manufacture) composed of a double envelope and of a stainless steel lid equipped with a butyl septum, a pH probe (Mettler Toledo), shaft with blades, 0.20 µm gas filters (Midisart, Sartorius) and different tubes for gas inlet, gas outlet, medium removal or addition. The reactor contained 2.5 L of MDT medium, except L-cysteine and glucose in order to prevent Maillard reactions, before being sterilized. After cooling down, 1 L of media was removed and the L-cysteine and the glucose, sterilized separately in solution of respectively 25 and 500

mL, were added sterilely in the reactor under nitrogen gas to reach MDT concentration. Inoculum (500 mL) cultured in 1 L bottle was then added in the bioreactor. Automatic addition of sterile KOH 3 N was used to control the pH, the temperature maintained at 30°C and the bioreactor was stirred at 100 rpm. Sequenced-batch operations were carried out by removing 40% (1 L) of the wasted liquid media under nitrogen overpressure. The reactor was refilled up to 2.5 L with sterile MDT medium containing 12.5 g of glucose (*i.e.* in order to obtain a concentration of 5 $g \cdot L^{-1}$ in the bioreactor).

2.4. Monitoring and analytical methods

The biogas produced in the BHP tests was collected daily during 96 hours by sterile syringe and needle pierced trough the butyl septum. Injections of the collected biogas in a 9N KOH measurement system for CO_2 sequestration allowed the determination of hydrogen content and volumetric hydrogen production by gas balance as already described by the authors (Hiligsmann *et al.*, 2011).

The 2.5L AnSBR was connected to a flow meter (TG05/5, Ritter) for continuous measurement of the biogas produced. The composition of the biogas was measured (or confirmed for the BHP tests) by a gas chromatography system (HP 8950 SeriesII) equipped with TCD detector, using nitrogen or helium as carrier gas (respectively for hydrogen and for nitrogen/methane/carbon dioxide detection) as fully described elsewhere (Hamilton *et al.*, 2010). Furthermore, the Gompertz model with the adjustment of three parameters (lag phase duration, maximum hydrogen production rate and maximum total hydrogen produced) was applied to the volumetric hydrogen production data following the method described by (Wang & Wan, 2009b).

The liquid culture samples were centrifuged at 13000 rpm for 3 min and the supernatants were filtered through a 0.2 µm cellulose acetate filter (Sartorius Minisart). The glucose, lactate,

formate, acetate, propionate, ethanol and butyrate were analyzed using a HPLC (Agilent 1100) equipped with a differential refraction index detector as described formerly by (Masset *et al.*, 2010). The concentrations measured in the culture medium were used to evaluate the carbon mass balance (MB) of glucose conversion in the soluble metabolites using the method of calculation reported by the authors (Hiligsmann *et al.*, 2011).

3. Results and discussion

3.1. Effect of encapsulated nanoparticles in BHP tests

3.1.1. Biological Hydrogen Potential

The production of hydrogen in *Clostridium butyricum* cultures supplemented with various encapsulated NP was investigated in BHP test (batch serum bottles of 200mL of liquid volume) (Hiligsmann *et al.*, 2011; Lin *et al.*, 2007). Four different elements were tested in triplicates series of bottles. The NP of 2-3 nm of diameter were encapsulated in a porous silica structure (Heinrichs *et al.*, 2008; Lambert *et al.*, 2004). The encapsulation of the NP in the silica matrix limits the risk of agglomeration of the active site. The NP concentration was adjusted at 10^{-6} mol·L^{-1} in the culture medium (Table 1). As a reference for the BHP test, a series was done without any catalyst supplementation (MDT medium only). Moreover, a negative control with porous SiO_2 particles without NP was carried out in order to assess the effect of the metallic (Pd, Ag or Cu) or metallic oxide (Fe_xO_y) active site on the production of hydrogen.

The volume of biogas was measured every 24 hours during four days after the inoculation. The daily volumetric hydrogen production, determined according to the description of the BHP tests in the section 2.3, was reported on the Figure 1. The hydrogen production profiles and total production were in line with previous BHP test with the *C. butyricum* strain (Hiligsmann *et al.*, 2011). A sigmoid profile was observed, indicating a lag phase followed by

exponential growth and simultaneous production of hydrogen. Indeed, when growing, the release of soluble metabolites in the medium decreased the pH down to inhibiting level. It resulted in lower hydrogen production after three days, near the end of the culture.

None of the NP tested showed an inhibiting effect since the production of hydrogen was similar or higher than in the reference BHP test (without NP and/or without SiO_2). Indeed, it is known that silver and copper behave as antimicrobial elements since they destruct the membrane cells by close contact between the microorganism and the NP (Bagchi et al., 2012; Sotiriou & Pratsinis, 2010). However, antimicrobial activity would not be effective in our experimentations because NP are encapsulated inside the porous silica matrix (Neal, 2008). By contrast, the addition of iron and copper induced a significant increase of the total hydrogen produced and different profiles of the cumulative curves in comparison with the reference BHP test (Table 2 and Figure 1). Both series with Fe/SiO_2 (synthesised by dissolution or cogelation method) and Cu/SiO_2 catalysts reached respectively 120 ± 5 and 104 ± 8 mL_{H2}, whereas the reference culture without catalyst produced 87 ± 7mL_{H2}. The highest performances for H_2 production were recorded with iron oxide NP suggesting the existence of interactions between NP and the bacteria and resulting in a faster hydrogen production. Furthermore, since the sole SiO_2 material (without NP) did not show any significant effect, it can be concluded that only the central active site (*i.e.* the metal or metal oxide NP) would play a role in the improvement of the hydrogen production.

3.1.2. <u>Hydrogen production rates and yields</u>

The Gompertz model was applied to the cumulative H_2 production curves. The resulting coefficients are reported in the Table 2. It confirms that the maximum cumulative H_2 productions were achieved for the iron oxide NP, *i.e.* 34% higher than in the reference BHP test. Moreover, the maximum hydrogen production rates (HPR) were 58 % higher with the

Fe/SiO_2 catalysts than the 1.97 ± 0.2 $mL \cdot h^{-1}$ recorded without catalyst addition. These results suggest that the NP have a higher influence on the kinetic of H_2 production than on the total volumetric production from glucose. By contrast, no significant influence was observed for the lag phase that varies between 7 and 14 hours for all the tests.

In addition, no significant difference was evidenced for the hydrogen production yields, based on the total hydrogen production and the substrate consumption (Table 2), *i.e.* respectively 1.08 ± 0.06, 0.96 ± 0.02 and 0.92 ± 0.04 $mol_{hydrogen}/mol_{glucose}$ for the cultures with Fe/SiO_2 catalyst, with the sole SiO_2 and without both of them.These yields are relatively low comparing to the literature (Lin et al., 2007; Wang & Wan, 2009a) since the pH was not controlled (decreasing from the initial pH set at 7.6 down to 4.7 ± 0.1 at the end of the experiments). Therefore, these experimentation conditions lead to large fluctuations in the metabolic activity and to a short time of culture at optimal pH for H_2 production (Hiligsmann *et al.*, 2011; Khanal *et al.*, 2004). It should be mentioned that, in anaerobic sequenced-batch reactors (AnSBR) with the pH set at optimal value of 5.2, the same strain of *C. butyricum* may produce hydrogen more efficiently reaching maximum yields of 2.3 $mol_{hydrogen}/mol_{glucose}$ (Masset *et al.*, 2010).

In our BHP tests, the gain of hydrogen production recorded with some catalysts was partially due to higher glucose consumption in these conditions than in the reference test. For instance with iron oxide NP, the yields were slightly increased by 12%, that is half of the increase in volumetric H_2 production. This is probably due to a different evolution of pH in these cultures since the production of hydrogen is a way for the bacteria to limit the pH decrease by the reduction of acidic proton into molecular hydrogen (Das, 2009). Therefore, the more the bacteria are producing hydrogen to limit the drop of pH, the more they can consume glucose for growth. The results about HPLC analysis of liquid samples (Figure 2) confirm that more glucose was consumed for the production of hydrogen with Fe/SiO_2 catalysts. Therefore, the

gain of hydrogen production was at least partially due to the increase of glucose consumption. Meanwhile, the yields were slightly increased of 12%, half of the increase performed for the volume of H_2.

3.1.3. Soluble metabolites distribution

Metabolites analysis (Figure 2) can be related to the low yields generally achieved in our BHP experiments since formate, lactate and ethanol were found in solution and are not related to metabolic pathways linked with the production of hydrogen. However, butyrate and acetate were respectively the second and the third major metabolites produced. According to literature, they are related with stoichiometric hydrogen yields of respectively 2 and 4 $mol_{hydrogen}/mol_{glucose}$. The metabolites profiles are in accordance with previous studies of *C. butyricum* cultured in batch experiment without pH control (Hiligsmann *et al.*, 2011; Lin *et al.*, 2007). The carbon mass balance (Figure 2) showed that the glucose was mostly converted in butyrate (around 40%), then in formate and lactate (respectively around 15 and 13.5%). In order to improve the production of hydrogen and direct the metabolism of the microorganisms toward the butyrate and acetate production, the pH should be controlled in continuous or semi-continuous fermentation.

The introduction of the NP in the media did not modify the metabolites profile. More glucose was consumed with Fe/SiO_2, Cu/SiO_2 and SiO_2 samples and less lactate was produced than in the reference triplicate. The same observation can be made for the carbon mass balance (Figure 2B), with a lower conversion of glucose in formate and lactate *i.e.* respectively 14 and 10% with Fe/SiO_2 catalysts. The changes in the metabolites profiles and carbon mass balance are of the same order than for the yields *i.e.* between 10 and 15%. These changes, taking into account the standard deviations obtained with the triplicates, should not be considered as

significant. Therefore, it can't be concluded that the NP lead to changes in the metabolic pathways followed by the bacteria but rather on the production rate of hydrogen.

All the results recorded for the BHP tests underline that interactions may exist between the bacteria and the iron oxide NP and may have an effect on the production of biohydrogen. However, in these experiments, since the pH evolved along the culture, it is hard to establish if the NP influenced the fermentation pathway (H_2 yields and metabolites) or only the kinetic for hydrogen production. Therefore, Fe/SiO_2 catalysts were used in an AnSBR in order to observe their effect on H_2 production in pH-controlled conditions.

3.2. Effect of iron oxide nanoparticles in AnSBR

3.2.1. Hydrogen production in the sequences without NP

An AnSBR was run over 14 sequences during 38 days in a 2.5 L tank reactor at a controlled pH of 5.2 ± 0.1 (*i.e.* the optimal pH for hydrogen production from glucose by *C. butyricum* (Masset *et al.*, 2010)). The sequenced-batch operations were carried out by sterile removal of the used medium (40% of working volume *i.e.* 1 L) and sterile addition of fresh media to reach $5 g \cdot L^{-1}$ of glucose. The first batch culture (F0) was followed by 6 sequences operated in classical conditions *i.e.* without NP (from F1 to F6). It allowed the establishment of stationary conditions for both H_2 production and soluble metabolites concentration. The effect of Fe/SiO_2 (dissol and cogel) catalyst was investigated in the further sequences with addition of iron NP at a concentration equal to 10^{-6} $mol_{Fe} \cdot L^{-1}$ at the beginning of the sequence F7 and F9.

The cumulated 15 sequences produced a total of 47.85 L of hydrogen in 39 days and between 3 and 3.3 L for each sequence. The hydrogen concentration in the biogas was measured at 54.8 ± 2.8 %. Since the first batch sequence (F0) was started without pH control (pH decreasing from 7.6 to 5.2 and then regulated), it produced only 1.7 L of hydrogen. This illustrates the importance of the pH regulation and the fundamental difference in experimental

conditions between the BHP tests and the sequences in AnSBR with pH control. By controlling the pH, the hydrogen production yields were improved from 1.2 to 2.2 ± 0.1 $mol_{hydrogen}/mol_{glucose}$ respectively for F0 and the following sequences (Figure 3). These performances are consistent with the results reported in similar conditions by (Masset *et al.*, 2010) However, the F0 sequence was important to promote bacteria growth (at a higher pH than 5.2) from only 0.5 L of inoculum added whereas the next sequences began with 1.5L of rich biomass culture medium (60% of the bioreactor medium from the former sequences).

In the successive sequences without NP, the yields did not show any significant variation. By contrast, the mean HPR showed an evolution. The mean HPR is estimated as the ratio between the volume of hydrogen produced and the total time of hydrogen production during the sequence. It should be noted that they were not calculated for F8, F11 and F14 since the elapsed production time for these sequences was overestimated. Figure 3 shows that it reached 65.8 $mL_{H2}\cdot h^{-1}$ for F1 and then decreased until F3. Indeed, considering the metabolites profiles on Figure 4, the stationary conditions were reached at F3 after an increase of butyrate and acetate concentrations, whereas unfavourable metabolites as formate, lactate and, in a lower extent, ethanol decreased below 7 $mmol\cdot L^{-1}$. A similar evolution of the metabolites profiles has already been discussed elsewhere and showed comparable metabolites distribution and concentrations (Masset *et al.*, 2010). Moreover, from F0 to F2, the total concentration of the metabolites in the culture medium was still at a low level that allowed the hydrogen production to occur rapidly without apparent inhibition. On the contrary, in stationary conditions without NP (from F3 to F7), the high concentration of butyrate and acetate seems to influence the hydrogen production that stabilized at a mean HPR of 44.7 ± 0.8 $mL_{H2}\cdot h^{-1}$ (Khanal et al., 2004; Wang & Wan, 2009a).

The carbon mass balance confirms that during sequences from F1 to F6 no significant changes occurred in the metabolic pathways in the sequenced-batch mode (Table 3). The

variations of metabolites concentration are then rather a consequence of the removal/addition operation than a change in the metabolic activity of the strain. Therefore, the batch sequence F0 and the two following sequences at controlled pH (F1 and F2) have to be considered as transition sequences. In the sequences F3 to F6, a stable production of hydrogen was observed without NP. These steady conditions enabled to test the effect of NP.

3.2.2. Hydrogen production in the sequences with NP addition

At the beginning of sequence F7 and F9, Fe/SiO_2 catalyst was added, each time at a final NP concentration of 10^{-6} mol·L^{-1}. The results show that the addition of iron oxide NP improved the mean HPR, from 44.7 ± 0.8 to 61.8 ± 3.9 $mL_{H2}·h^{-1}$, whereas the yields remained at 2.2 ± 0.1 $mol_{hydrogen}/mol_{glucose}$. (Figure 3). Therefore, the addition of NP would have a kinetic effect rather than a metabolic effect on the production of hydrogen. It played a role on the rate of hydrogen formation rather than on the metabolites pathways followed by the bacteria, as already underlined in the BHP tests. These higher HPR were similar in the sequences from the sequences F7 and F9 to F14 though the NP concentration decreased progressively due to addition/removal of culture medium at the beginning of each sequences without NP addition. Indeed it is considered that with the successive dilutions of the medium the concentration of NP was ten times lower in F14 than in F9.

A Gompertz modelling on the production of hydrogen was performed for each sequence with at least three volumetric data points (Figure 6). It confirmed the former observation about the mean HPR and that the effect of NP on the HPR did not decreased with the successive dilutions after F9.The maximum HPR reached a stable value after F3 in relation with the stabilization of the AnSBR. The mean values without NP from F3 to F6 reached a maximum HPR of 98.9 ± 9.6 $mL_{H2}·h^{-1}$. The increase of the rate brought by the addition of NP is confirmed with a maximum HPR from F7 to F14 of 214.5 ± 33.9 $mL_{H2}·h^{-1}$. By contrast, the

maximum volume of hydrogen estimated by the Gompertz model slightly decreased from 3.35 ± 0.11 to 3.15 ± 0.22 L_{H2} per sequence.

The metabolic profiles and carbon mass balance did not show any significant differences between the sequences without and with NP (Table 3). In both case, butyrate and acetate were the major metabolites, respectively at mean values of 10.2 and 18.3 $mmol \cdot L^{-1}$ produced during each sequence. The other metabolites found at lower concentration were lactate, formate and ethanol, at respectively 0.5, 1.8 and 0.4 $mmol \cdot L^{-1}$. These values are in accordance with previous studies in similar conditions (Masset *et al.*, 2010). At optimal pH conditions, the metabolic pathway was clearly oriented toward the production of hydrogen allowing higher yields. This is shown with more than 42% of the carbon consumed converted in butyrate and 13% in acetate.

Regarding the mechanisms promoted by the NP, it can be suggested that they were not metabolised by the bacteria but played a role of active catalytic site involved in the production of hydrogen. It is known that the hydrogen-producing bacteria need iron as a cofactor for hydrogenases synthesis (Chong et al., 2009; Karadag & Puhakka, 2010; Lee et al., 2001). These authors evaluated the minimal iron requirement for the bacterial growth at 10^{-5} $mol \cdot L^{-1}$, but showed that the production of hydrogen could be enhanced by 5 to 10 times by increasing the concentration by a hundred to a thousand time. In comparison, the amount of iron added in our experimentations in the NP form is about 10-fold lower and decreases after successive sequences. On the one hand, a very low amount of iron was added with the NP and diluted with successive sequences. On the other hand, external iron ions were also contained as trace elements in the compounds contained in the culture medium. The iron concentration is estimated at $2 \cdot 10^{-5}$ $mol \cdot L^{-1}$ (Abelovska *et al.*, 2007). Therefore the total amount of iron oxide NP added at F9 represent only 7% of the iron source available in the nutrients. Furthermore, it is more likely that the bacteria would consume the free ions from the medium before trying to

use the stable iron oxide NP encapsulated inside the porous silica matrix. Moreover, it has been shown that free iron supplemented in the media had a clear effect on the rates rather than on the yields as it was observed in this study (Hamilton *et al.*, 2010).

3.3. General discussion

The effects of zero-valent gold NP were demonstrated on fermentative bioH_2 production by (Zhang & Shen, 2007). They showed that the H_2 production increases with the decrease of NP size. The concentration of gold NP used by these authors (10^{-8} mol·L^{-1}) was a hundred fold lower than the concentration used in this work. In comparison with this work, 9 sequenced-batch operations after F9 should be achieved to reach the same concentration. Furthermore, the nature of NP in the Fe/SiO_2 catalysts used in our study has been determined as mainly non-reduced iron oxide Fe_2O_3 (Heinrichs *et al.*, 2008). Therefore, considering the low concentration of NP and their ferric oxide state, it is suggested that the enhancement of the production of hydrogen with Fe/SiO_2 catalysts is related to a catalytic activity working in parallel with the enzymes involved in electron transfer as the hydrogenases, *c*-cytochromes or/and with extracellular electron mediators. Indeed, the immobilized iron oxide active sites could be used by the bacteria for oxidation/reduction chemical reaction (considering the redox couple Fe^{2+}/Fe^{3+}) to help the bacteria transferring faster its electrons without consuming or metabolising the iron as when it is added to the medium in a dissolved form. However, considering the small size of the iron oxide NP (around 3 nm), the surface effect is greatly enhanced and may improve the ability of the NP to react with the electrons transported by mediators and to transfer them efficiently to electron acceptors or eventually protons.

C. butyricum is able transfer electrons out of the cell. Indeed, it is known to have *c*-type cytochromes on the outer cell surface (Park *et al.*, 2001). In addition, interactions and electron transfers between *Clostridium* bacteria strains and metallic elements have already been

supposed in microbial fuel cells (MFC) where clostridia strains have often been isolated and identified (Lovley, 2008; Park *et al.*, 2001). Therefore the NP would act as a chemical catalyst and may add efficiency in the biochemical hydrogen production process usually mediated by the sole enzymes in the cells for the production of hydrogen through the reduction of protons.

Furthermore, the hypothesised mechanism also suggests an efficient diffusion of mediating-molecules in the porous structure of the encapsulating-silica. A similar diffusion process was demonstrated in the catalyst characterization by the authors (Heinrichs *et al.*, 2008; Lambert *et al.*, 2004). Indeed, the pore size ranges from two to several hundred nanometres. Therefore the pores would connect the outer medium of the silica matrix to the central iron oxide active site. It reinforces the assumption of mediated processes since the bacteria should not come directly in contact with the iron NP. Therefore it should use a redox intermediate to transport the electron from the cell surface to the active metallic oxide surface.

The precise role of iron oxide NP, their mechanism of action and their potential influence on the enzymatic activity will have to be investigated and confirmed in further work and will focus on links with hydrogenases activity and electron transfer mechanisms. The hypothesis of partial NP dissolution in the liquid medium has not been ruled out and attention should be brought to this subject in future studies. Indeed, if partial dissolution would occur, its proportion should be measured. However, in the experiments carried out here no lowering effect was observed with successive sequences in the AnSBR . This work also opens the way to researches about combined catalytic and biological treatment for the bioremediation of soil pollution with substances such as aromatic or chlorinated compounds, since mechanism of electron transfer are highly important in such processes.

4. <u>Conclusions</u>

This study leads to a successful improvement of the biohydrogen production process by *C. butyricum* combined with encapsulated iron oxide NP added at very low amount (10^{-6} mol·L^{-1}). Interactions with NP have been assumed since an enhancement of the HPR has been achieved. The production rates were improved by 38 and 113% in the batch or AnSBR mode respectively. By contrast, no significant change in the metabolic pathways was observed, regarding the H_2 yields and soluble metabolites distribution. The addition of the NP would improve the hydrogen production made by the bacteria trough catalytic mechanism involving extra-cellular mediated-molecules.

5. Acknowledgements

L. Beckers and S. D. Lambert are grateful to the F.R.S.-FNRS (Fond National pour la Recherche Scientifique) of Belgium for supporting their work and researches as respectively Research fellow and Research associate. This work was also funded through an ARC grant provided by the French Community of Belgium (ARC-07/12-04).

6. References

Abelovska, L., Bujdos, M., Kubova, J., Petrezselyova, S., Nosek, J., Tomaska, L. 2007. Comparison of element levels in minimal and complex yeast media. *Canadian Journal of Microbiology*, **53**(4), 533-535.

Bagchi, B., Dey, S., Bhandary, S., Das, S., Bhattacharya, A., Basu, R., Nandy, P. 2012. Antimicrobial efficacy and biocompatibility study of copper nanoparticle adsorbed mullite aggregates. *Materials Science and Engineering C*, **32**(7), 1897-1905.

Chong, M.L., Rahman, N.A., Yee, P.L., Aziz, S.A., Rahim, R.A., Shirai, Y., Hassan, M.A. 2009. Effects of pH, glucose and iron sulfate concentration on the yield of biohydrogen by Clostridium butyricum EB6. *International Journal of Hydrogen Energy*, **34**(21), 8859-8865.

Das, D. 2009. Advances in biohydrogen production processes: An approach towards commercialization. *International Journal of Hydrogen Energy*, **34**(17), 7349-7357.

Davila-Vazquez, G., Arriaga, S., Alatriste-Mondragon, F., de Leon-Rodriguez, A., Razo-Flores, E. 2008. Fermentative biohydrogen production: trends and perspectives. *Reviews in Environmental Science and Bio/Technology*, **7**(1), 27-45.

Dinesh, R., Anandaraj, M., Srinivasan, V., Hamza, S. 2012. Engineered nanoparticles in the soil and their potential implications to microbial activity. *Geoderma*, **173–174**(0), 19-27.

Grieger, K.D., Fjordbøge, A., Hartmann, N.B., Eriksson, E., Bjerg, P.L., Baun, A. 2010. Environmental benefits and risks of zero-valent iron nanoparticles (nZVI) for in situ remediation: Risk mitigation or trade-off? *Journal of Contaminant Hydrology*, **118**(3-4), 165-183.

Hallenbeck, P.C. 2009. Fermentative hydrogen production: Principles, progress, and prognosis. *International Journal of Hydrogen Energy*, **34**(17), 7379-7389.

Hamilton, C., Hiligsmann, S., Beckers, L., Masset, J., Wilmotte, A., Thonart, P. 2010. Optimization of culture conditions for biological hydrogen production by *Citrobacter freundii* CWBI952 in batch, sequenced-batch and semicontinuous operating mode. *International Journal of Hydrogen Energy*, **35**(3), 1089-1098.

Heinrichs, B., Pirard, J.-P., Schoebrechts, J.-P. 2001. Mass transfer in low-density xerogel catalysts. *AIChE Journal*, **47**(8), 1866-1873.

Heinrichs, B., Rebbouh, L., Geus, J.W., Lambert, S., Abbenhuis, H.C.L., Grandjean, F., Long, G.J., Pirard, J.-P., van Santen, R.A. 2008. Iron(III) species dispersed in porous silica through sol–gel chemistry. *Journal of Non-Crystalline Solids*, **354**(2–9), 665-672.

Hiligsmann, S., Masset, J., Hamilton, C., Beckers, L., Thonart, P. 2011. Comparative study of biological hydrogen production by pure strains and consortia of facultative and strict anaerobic bacteria. *Bioresource Technology*, **102**(4), 3810-3818.

Holladay, J.D., Hu, J., King, D.L., Wang, Y. 2009. An overview of hydrogen production technologies. *Catalysis Today*, **139**(4), 244-260.

Jagadevan, S., Jayamurthy, M., Dobson, P., Thompson, I.P. 2012. A novel hybrid nano zerovalent iron initiated oxidation – Biological degradation approach for remediation of recalcitrant waste metalworking fluids. *Water Research*, **46**(7), 2395-2404.

Karadag, D., Puhakka, J.A. 2010. Enhancement of anaerobic hydrogen production by iron and nickel. *International Journal of Hydrogen Energy*, **35**(16), 8554-8560.

Kato, S., Hashimoto, K., Watanabe, K. 2012. Microbial interspecies electron transfer via electric currents through conductive minerals. *Proceedings of the National Academy of Sciences*, **109**(25), 10042-10046.

Khanal, S.K., Chen, W.H., Li, L., Sung, S.W. 2004. Biological hydrogen production: effects of pH and intermediate products. *International Journal of Hydrogen Energy*, **29**(11), 1123-1131.

Klavsyuk, A.L., Kolesnikov, S.V., Gainullin, I.K., Saletsky, A.M. 2011. Study of the interaction of a palladium nanocontact with a hydrogen molecule. *JETP Letters*, **93**(9), 530-533.

Korbekandi, H., Iravani, S., Abbasi, S. 2009. Production of nanoparticles using organisms. *Critical Reviews in Biotechnology*, **29**(4), 279-306.

Kothari, R., Singh, D.P., Tyagi, V.V., Tyagi, S.K. 2012. Fermentative hydrogen production – An alternative clean energy source. *Renewable and Sustainable Energy Reviews*, **16**(4), 2337-2346.

Lambert, S., Alié, C., Pirard, J.-P., Heinrichs, B. 2004. Study of textural properties and nucleation phenomenon in Pd/SiO2, Ag/SiO2 and Cu/SiO2 cogelled xerogel catalysts. *Journal of Non-Crystalline Solids*, **342**(1–3), 70-81.

Lee, Y.J., Miyahara, T., Noike, T. 2001. Effect of iron concentration on hydrogen fermentation. *Bioresource Technology*, **80**(3), 227-231.

Lin, P.Y., Whang, L.M., Wu, Y.R., Ren, W.J., Hsiao, C.J., Li, S.L., Chang, J.S. 2007. Biological hydrogen production of the genus *Clostridium*: Metabolic study and mathematical model simulation. *International Journal of Hydrogen Energy*, **32**, 1728-1735.

Lovley, D.R. 2008. The microbe electric: conversion of organic matter to electricity. *Current Opinion in Biotechnology*, **19**(6), 564-571.

Marban, G., Vales-Solis, T. 2007. Towards the hydrogen economy? *International Journal of Hydrogen Energy*, **32**(12), 1625-1637.

Masset, J., Hiligsmann, S., Hamilton, C., Beckers, L., Franck, F., Thonart, P. 2010. Effect of pH on glucose and starch fermentation in batch and sequenced-batch mode with a recently isolated strain of hydrogen-producing *Clostridium butyricum* CWBI1009. *International Journal of Hydrogen Energy*, **35**(8), 3371-3378.

Neal, A. 2008. What can be inferred from bacterium–nanoparticle interactions about the potential consequences of environmental exposure to nanoparticles? *Ecotoxicology*, **17**(5), 362-371.

Park, H.S., Kim, B.H., Kim, H.S., Kim, H.J., Kim, G.T., Kim, M., Chang, I.S., Park, Y.K., Chang, H.I. 2001. A Novel Electrochemically Active and Fe(III)-reducing Bacterium Phylogenetically Related to Clostridium butyricum Isolated from a Microbial Fuel Cell. *Anaerobe*, **7**(6), 297-306.

Sagnak, R., Kapdan, I.K., Kargi, F. 2010. Dark fermentation of acid hydrolyzed ground wheat starch for bio-hydrogen production by periodic feeding and effluent removal. *International Journal of Hydrogen Energy*, **35**(18), 9630-9636.

Sotiriou, G.A., Pratsinis, S.E. 2010. Antibacterial Activity of Nanosilver Ions and Particles. *Environmental Science & Technology*, **44**(14), 5649-5654.

Wang, J.L., Wan, W. 2009a. Factors influencing fermentative hydrogen production: A review. *International Journal of Hydrogen Energy*, **34**(2), 799-811.

Wang, J.L., Wan, W. 2009b. Kinetic models for fermentative hydrogen production: A review. *International Journal of Hydrogen Energy*, **34**(8), 3313-3323.

Xu, S., Liu, H., Fan, Y., Schaller, R., Jiao, J., Chaplen, F. 2012. Enhanced performance and mechanism study of microbial electrolysis cells using Fe nanoparticle-decorated anodes. *Applied Microbiology and Biotechnology*, **93**(2), 871-880.

Zhang, Y.F., Shen, J.Q. 2007. Enhancement effect of gold nanoparticles on biohydrogen production from artificial wastewater. *International Journal of Hydrogen Energy*, **32**(1), 17-23.

Zidansek, A., Blinc, R., Jeglic, A., Kabashi, S., Bekteshi, S., Slaus, I. 2009. Climate changes, biofuels and the sustainable future. *International Journal of Hydrogen Energy*, **34**(16), 6980-6995.

Figure captions

Figure 1: Cumulative volume of hydrogen production by the pure *C. butyricum* in BHP tests with 10^{-6} mol·L^{-1} of encapsulated metallic NP. The volumes of hydrogen are calculated at atmospheric pressure and 30°C. The standard deviation bars are calculated on the triplicate experiments made for each condition.

Figure 2: Investigation of hydrogen production by the pure *C. butyricum* in BHP tests with metallic NP. (A) Metabolites analysis (mmol·L^{-1}) at the end of the fermentation (96h). (B) Carbon mass balance (%).The standard deviation bars are calculated on the triplicate experiments made for each condition.

Figure 3: Yields and mean hydrogen production rates in 2.5 L AnSBR with *C. butyricum* and investigation on the effect of the addition of metallic NP. The Fe/SiO_2 NP were added at the sequence 7 and 9. HPR produced calculated at atmospheric pressure and 30°C.

Figure 4: Evolution of the metabolites concentration during the investigation on the effect of Fe/SiO_2 NP added at the sequence 7 and 9 in the 2.5 L AnSBR on the production of hydrogen by *C. butyricum*.

Figure 5: Application of the Gompertz model on the hydrogen production in the 2.5 L AnSBR with Fe/SiO_2 NP. (A) Gompertz coefficients adjusted for each sequence with at least three values measured and (B) mean Gompertz coefficients for the sequences without NP (F3 to F6) and with NP (F7 to F14).

Table 1: Characteristics of the catalyst samples: preparation method, metal loading in catalyst; catalyst mass and volume of suspension used in the MDT medium to reach the final metallic concentration of 10-6 mol_{metal}·L^{-1}

Table 2: Hydrogen yields and Gompertz coefficient adjusted on the profiles of volumetric hydrogen production curves for the BHP tests with NP. Standard deviations are calculated on the triplicates experiments made for each condition. All the R^2 for the Gompertz model were higher than 0.999.

Table 3: Comparison of the metabolites and CO_2 mass balance of the successive sequences without and with Fe/SiO_2 NP in the 2.5 L AnSBR. The NP were added at the sequences F7 and F9. Negative values correspond to a consumption of the metabolite.

Table 1: Metal loading in catalyst; catalyst mass and volume of suspension used in the MDT medium to reach the final metallic concentration of 10^{-6} $mol_{metal} \cdot L^{-1}$

NP denotation	Reference sample	Reduction of the sample	Metallic mass content	Mass of catalyst added in 50mL of water for concentrated suspension preparation (g)	Volume of concentrated NP suspension added in 1 L of MDT medium (mL)
SiO2	X3 (Lambert et al., 2004)	No	-	0.2034	1.25
Pd/SiO2	Pd3.1 (Lambert et al., 2004)	Yes	3.12%	0.0645	2.5
Ag/SiO2	Ag1.5 (Lambert et al., 2004)	Yes	1.54%	0.0506	6.25
Fe/SiO2 dissol	Fe/SiO2-D (Heinrichs et al., 2008)	No	1.65%	0.1354	1.25
Fe/SiO2 cogel	Fe/SiO2-C(E) (Heinrichs et al., 2008)	No	1.65%	0.1354	1.25
Cu/SiO2	Cu0.1 (Lambert et al., 2004)	Yes	0.12%	0.2059	12.5

Table 2: Hydrogen yields and Gompertz coefficient adjusted on the profiles of volumetric hydrogen production curves for the BHP tests with NP. Standard deviations are calculated on the triplicates experiments made for each condition. All the R^2 for the Gompertz model were higher than 0.999.

	Yields ($mol_{H2} \cdot mol_{glucose}^{-1}$)	Gompertz model		
		Lag phase duration (h)	Maximum H_2 production rate ($mL_{H2} \cdot h^{-1}$)	Total hydrogen production (mL_{H2})
Reference	0.92 ± 0.08	11.2 ± 1.6	1.97 ± 0.24	86.7 ± 7
Pd/SiO_2	0.97 ± 0.09	11.5 ± 0.8	2.33 ± 0.22	95.8 ± 8.5
Ag/SiO_2	0.97 ± 0.02	11.8 ± 1.8	2.21 ± 0.17	93.8 ± 2.8
Fe/SiO_2 dissol	1.08 ± 0.06	11.6 ± 4.2	3.49 ± 0.31	119.4 ± 5.8
Fe/SiO_2 cogel	1.05 ± 0.01	9.1 ± 1.9	2.85 ± 0.15	113.3 ± 1.3
Cu/SiO_2	1.01 ± 0.08	8.3 ± 2.1	2.4 ± 0.6	103.9 ± 7.9
SiO_2	0.96 ± 0.02	12.8 ± 3.1	2.13 ± 0.7	97.3 ± 2.7

Table 3: Comparison of the metabolites and CO_2 mass balance of the successive sequences without and with Fe/SiO_2 NP in the 2.5 L AnSBR. The NP were added at the sequences F7 and F9. Negative values correspond to a consumption of the metabolite.

	Carbon converted from glucose (%)					
	Lactate	Formate	Acetate	Ethanol	Butyrate	CO_2
F1	-3.9	-0.8	13.4	1.1	55.7	26.2
F2	0	0.2	14	0.5	49.2	24.9
F3	0	0.2	14.3	0.5	51.2	25
F4	0	1.1	13.1	0.5	48.8	23.6
F5	0	0.6	13	0.42	47.7	25.6
F6	1.2	1.5	14.7	1.4	48.6	25.9
F7	2.1	1.4	14.2	1	43.9	24.7
F8	1.9	1.5	14	1.5	46.5	26.7
F9	1	0.5	14.4	2.2	44.8	24.1
F10	2.4	0.9	13.8	1.6	42.7	24.1
F11	1.5	2.4	14.1	1.5	42.9	23.8
F12	4	1.5	13.6	0.1	42.5	23.8
F13	2.8	4.0	14.5	1.1	45.7	23.9
F14	2.6	2.8	14.6	2.6	42.8	24.3
Mean value without NP (F3 – F6)	0.3 ± 0.6	0.8± 0.6	13.8 ± 0.8	0.5 ± 0.1	49.1 ± 1.5	25 ± 1
Mean value with NP (F7 – F14)	2.7 ± 1	2.7 ± 1	14.2 ± 0.5	1.3 ± 1	43.5 ± 1.5	23.9 ± 0.2

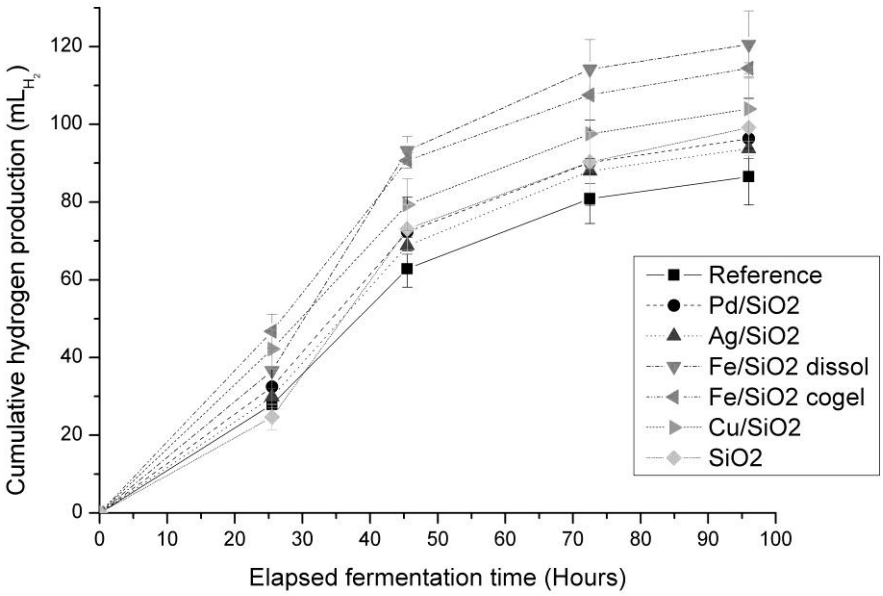

Figure 1: Investigation of hydrogen production by the pure *C. butyricum* in BHP tests with 10^{-6} mol·L^{-1} of encapsulated metallic NP. The volumes of hydrogen are calculated at atmospheric pressure and 30°C. The standard deviation bars are calculated on the triplicate experiments made for each condition.

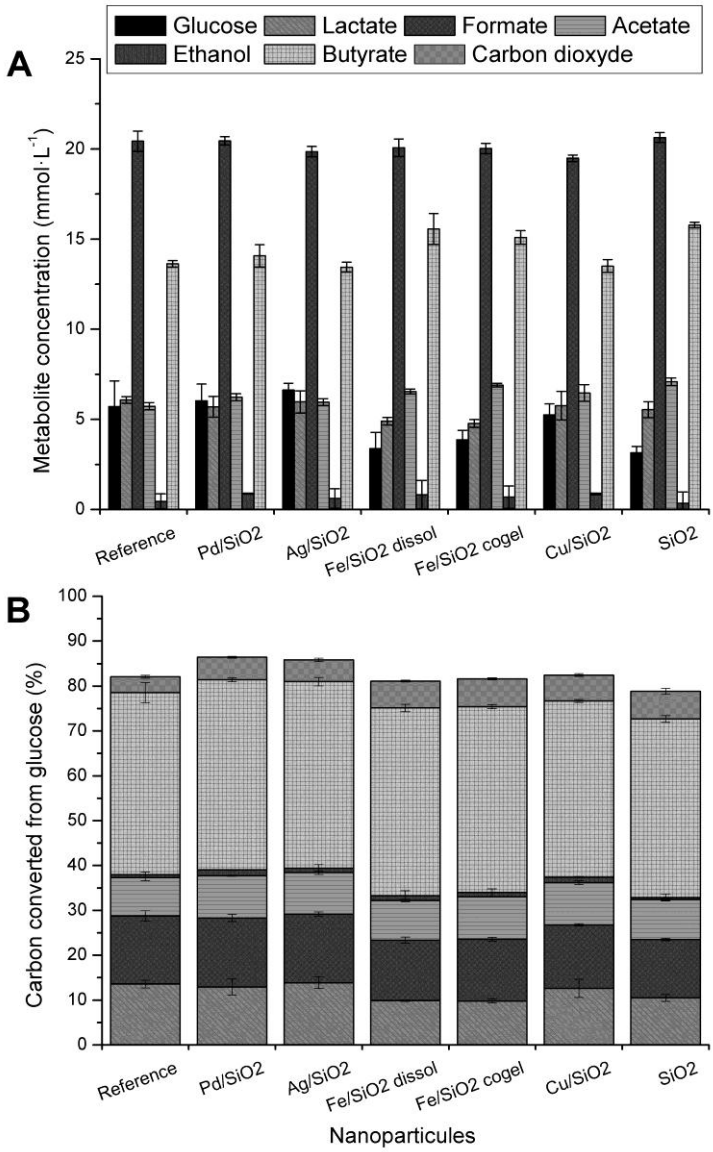

Figure 2: Investigation of hydrogen production by the pure *C. butyricum* in BHP tests with metallic NP. (A) Metabolites analysis (mmol·L^{-1}) at the end of the fermentation (96h). (B) Carbon mass balance (%).The standard deviation bars are calculated on the triplicate experiments made for each condition.

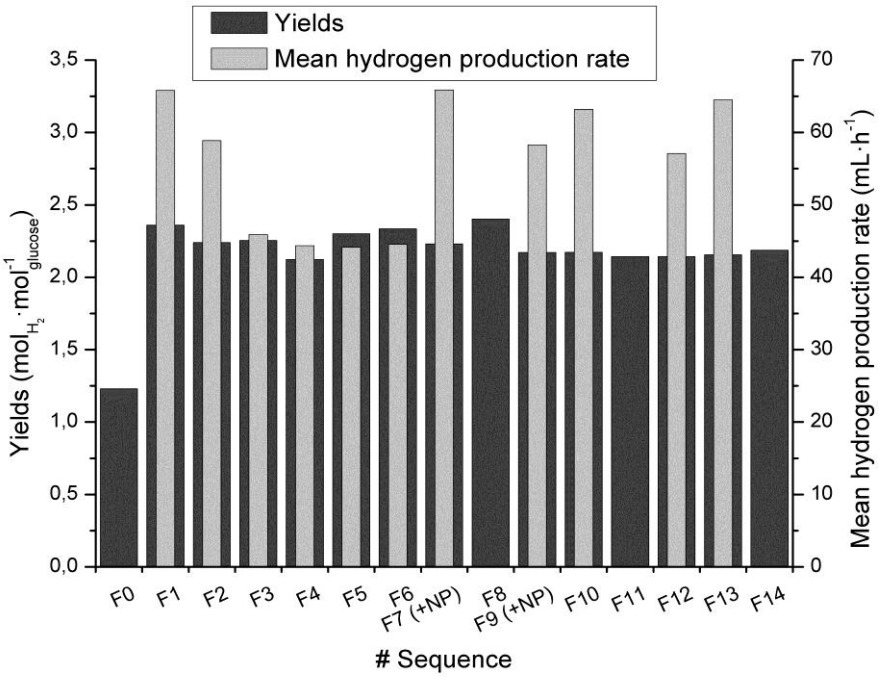

Figure 3: Yields and mean hydrogen production rates in 2.5 L AnSBR with *C. butyricum* and investigation on the effect of the addition of metallic NP. The Fe/SiO_2 NP were added at the sequence 7 and 9. HPR produced calculated at atmospheric pressure and 30°C.

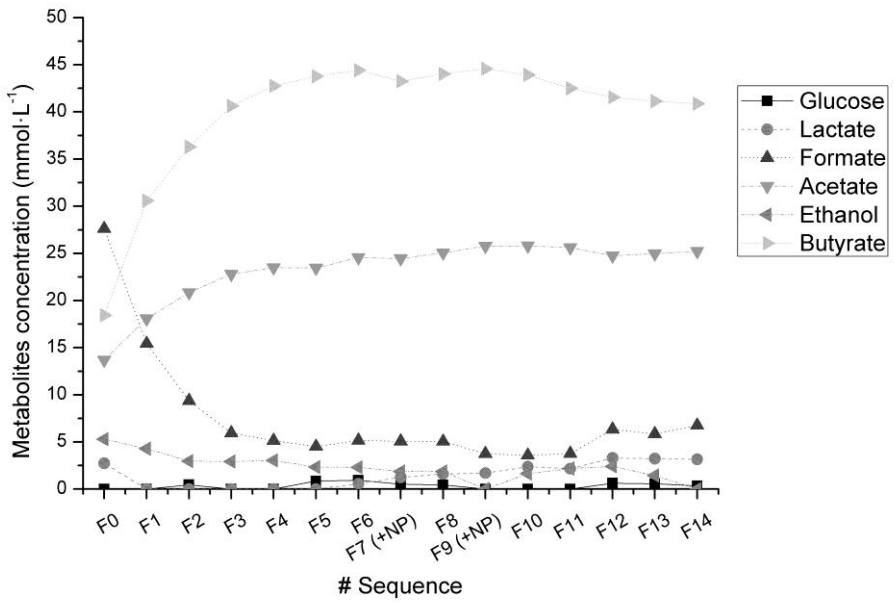

Figure 4: Evolution of the metabolites concentration during the investigation on the effect of Fe/SiO_2 NP added at the sequence 7 and 9 in 2.5 L AnSBR on the production of hydrogen by *C. butyricum*.

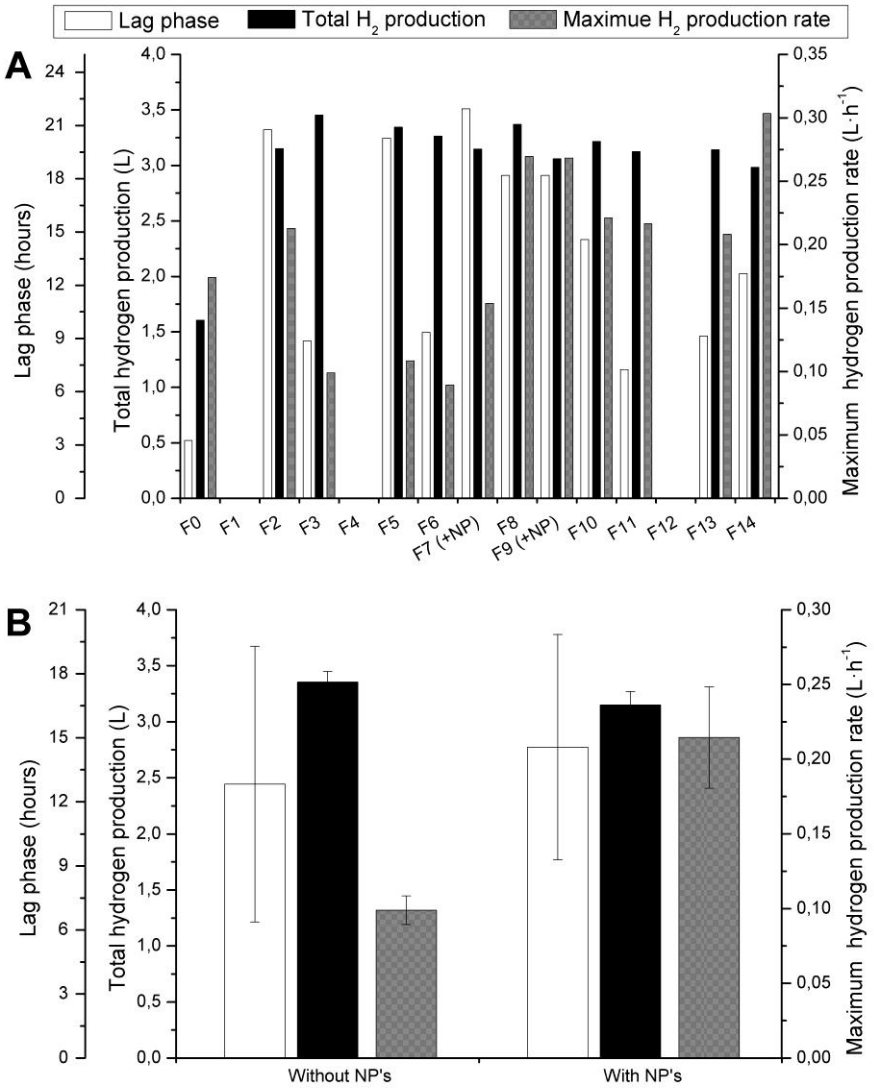

Figure 5: Application of the Gompertz model on the hydrogen production in the 2.5 L AnSBR with Fe/SiO_2 NP. (A) Gompertz coefficients adjusted for each sequence with at least three values measured and (B) mean Gompertz coefficients for the sequences without NP (F3 to F6) and with NP (F7 to F14).